

Orbital magnetic moment and extrinsic spin Hall effect for iron impurities in gold

Alexander B. Shick,¹ Jindřich Kolorenč,^{2,1} Václav Janiš,¹ and Alexander I. Lichtenstein²

¹*Institute of Physics, Academy of Sciences of the Czech Republic, Na Slovance 2, CZ-182 21 Prague, Czech Republic*

²*Institute of Theoretical Physics, University of Hamburg, Jungiusstraße 9, D-20355 Hamburg, Germany*

(Received 9 August 2011; published 28 September 2011)

We report electronic structure calculations of an iron impurity in a gold host. The spin, orbital, and dipole magnetic moments were investigated using the local density approximation (LDA) + U correlated band theory. We show that the *around-mean-field* LDA + U reproduces the x-ray magnetic circular dichroism (XMCD) experimental data well and does not lead to the formation of a large orbital moment on the Fe atom. Furthermore, exact diagonalization of the multiorbital Anderson impurity model with the full Coulomb interaction matrix and the spin-orbit coupling is performed in order to estimate the spin Hall angle. The obtained value $\gamma_S \approx 0.025$ suggests that there is no giant extrinsic spin Hall effect due to scattering on iron impurities in gold.

DOI: [10.1103/PhysRevB.84.113112](https://doi.org/10.1103/PhysRevB.84.113112)

PACS number(s): 72.25.Ba, 71.15.Rf, 71.70.Ej, 85.75.-d

During the last several years, broad interest and attention have been devoted to the spin Hall effect (SHE) in semiconductors¹ and metals.² This effect amounts to an observation of a transversal spin current when a charge current is flowing through a solid. The SHE is caused by the spin-orbit coupling (SOC) and can occur even in nonmagnetic solids.²

Recently, an experimental observation of a giant SHE in Au/FePt has been reported.³ A spin Hall conductivity of $\sim 10^5 \Omega^{-1} \text{cm}^{-1}$ and a spin Hall angle as large as ~ 0.1 were measured.³ Guo *et al.* suggested the effect to be of extrinsic origin due to the Fe and Pt impurities in gold.⁴ They reported a local (spin) density approximation (LSDA) plus Coulomb U (LDA + U) solution for Fe in Au with a very large orbital magnetic moment $M_L \sim 1.5\mu_B$.

The results of Ref. 4 contradict the LDA + U calculations presented in Ref. 5, which reported a tiny $M_L \sim 0.02\mu_B$. The value of M_L from Ref. 4 is clearly inconsistent with the experimental x-ray magnetic circular dichroism (XMCD) data for the ratio of M_L and the effective spin moment M_S , $R_{LS} = 0.034$.⁶ Assuming $M_S \sim 3\mu_B$ leads to $M_L \sim 0.1\mu_B$, which is an order of magnitude smaller than the prediction of Ref. 4. It was suggested⁷ that the discrepancy between Refs. 4 and 5 is due to different choices of the Coulomb U . A large value of M_L is calculated with $U = 5 \text{ eV}$ (Ref. 4), while much smaller ones are obtained with $U = 3 \text{ eV}$.⁵

In this work we revisit the electronic and magnetic structure of the Fe impurity in Au. We examine different flavors of the rotationally invariant LDA + U method:⁸ the “fully localized limit” (FLL) as well as the “around mean field” (AMF) version. The results for the orbital magnetic moment M_L are compared with the available experimental data.

Both LSDA and LDA + U methods yield broken-symmetry static-mean-field solutions with ordered spin and orbital moments, whereas the true dynamical solution of an impurity in a nonmagnetic host exhibits $M_S = 2\langle \hat{S}_z \rangle = 0$ and $M_L = \langle \hat{L}_z \rangle = 0$ when no external magnetic field is applied and no preferential direction for the orientation of the moments exists. In order to go beyond the static mean field and to incorporate the dynamical electron correlations, we employ the exact diagonalization (ED) method to solve a multiorbital single impurity Anderson model (SIAM)⁹ whose parameters are extracted from LDA calculations. We evaluate the spectral

density at the Fe impurity in Au and estimate the spin Hall angle due to skew scattering on the impurity. A relation between the electronic structure and the extrinsic SHE is discussed.

As a computational model we use an FeAu₁₅ supercell chosen to keep Fe and its 12 nearest Au neighbors separated from other impurity atoms. No relaxation is performed as it is not essential for the close-packed *fcc* structure. We use the lattice constant of elemental Au, $a = 7.71 \text{ a.u.}$ All calculations are performed making use of a relativistic version (with SOC) of LDA + U implemented in the full-potential linearized augmented plane wave (FP-LAPW) basis.¹⁰ The radii of the atomic muffin-tin (MT) spheres are set to 2.3 a.u. (Fe) and 2.5 a.u. (Au). The parameter $R \times K_{\text{max}} = 7.6$ determined the basis set size, and the Brillouin zone was sampled with 343 k points. We checked that a finer sampling with 729 k points does not modify the results.

First, we apply the conventional LSDA with the von Barth and Hedin¹¹ exchange-correlation potential implemented within the relativistic FP-LAPW method.¹² Our results for the spin and orbital moments inside the Fe MT sphere, M_S and M_L , are compared with the results of other calculations in Table I. In spite of a relatively small (16 atoms only) and unrelaxed supercell, the present results are in fair agreement with VASP⁵ results for a substantially larger and relaxed supercell containing 108 atoms, with the tight-binding linear muffin-tin orbital (TB-LMTO) results for a 55 atom supercell,¹³ and with the Korringa-Kohn-Rostoker atomic-sphere approximation (KKR-ASA) calculations.¹⁴ All calculations indicate a small value of M_L for Fe impurity in Au, which is typical for 3d transitional metals and alloys. The calculated M_L/M_S ratio is substantially smaller than the experimental value $R_{LS} = 0.034$.⁶ Typically, M_L is underestimated in LSDA due to the lack of orbital polarization. This leads to a smaller ratio M_L/M_S and explains the disagreement with experiment.

The calculated d -orbital density of states (DOS) for an Fe atom and the first nearest-neighbor Au atoms are shown in Fig. 1 (top). LSDA yields fully occupied Fe spin-up states that are hybridized with shallow Au d states. The Fe spin-down states are substantially more localized. Analysis of the projected DOS shows that the e_g -like ($d_{x^2-y^2} + d_{3z^2-r^2}$) states become practically fully spin polarized, while the t_{2g} -like

TABLE I. LSDA magnetic moments on Fe in Au (in units of μ_B).

FeAu ₁₅	M_S	M_L	M_L/M_S
FP-LAPW	3.04	0.024	0.008
VASP (Ref. 5)	3.08	0.040	0.012
TB-LMTO (Ref. 13)	2.95	0.008	0.003
KKR-ASA (Ref. 14)			0.007

($d_{xy} + d_{zx} + d_{zy}$) states are only partially polarized; see Fig. 1 (top).

Now we turn to the LDA + U calculations. We compare FLL and AMF variants of the rotationally invariant LDA + U method. The full local occupation matrix with all spin off-diagonal components is preserved. The double counting of the nonspherical d -state contributions to the LSDA and the LDA + U parts of the potential is corrected. The exchange $J = 0.9$ eV was used for Fe (Slater integrals $F_2 = 7.75$ eV, $F_4 = 4.85$ eV). The Coulomb U was varied from 3 to 5 eV.

The spin M_S , orbital M_L , and dipole M_D (Ref. 15) $3d$ magnetic moments are given in Table II together with the occupation of the Fe atom d orbitals, n_d . Both FLL and AMF

TABLE II. Magnetic moments (in μ_B) and $3d$ occupation n_d of the Fe impurity in Au host as a function of Coulomb U .

FeAu ₁₅	FLL			AMF	
	3	4	5	3	4
U (eV)					
M_S	3.18	3.21	3.29	2.94	2.90
M_L	1.24	1.36	1.44	0.16	0.22
$7M_D$	2.36	2.71	3.57	2.16	2.35
R_{LS}	0.23	0.23	0.21	0.03	0.04
n_d	6.00	6.00	5.97	6.03	6.03

flavors of LDA + U lead to an enhancement of M_L with respect to the LSDA estimate. It is due to nonspherical Coulomb and exchange interactions, which are incorporated in LDA + U (Ref. 16) and cause an additional orbital polarization to that induced by the spin-orbit coupling. The value of M_L increases with the increase of the Coulomb U . It is observed that the FLL double counting yields a substantially stronger enhancement of M_L than the AMF method.

There is also a substantial magnetic dipole moment M_D formed on the Fe impurity. When the spin-orbit coupling is included and spin polarization is allowed, the initial cubic symmetry is broken, and only the tetragonal symmetry remains. This effect is rather small in LSDA. It becomes substantially enhanced in LDA + U due to the additional orbital polarization. This effect is visible on the AMF LDA + U DOS shown in Fig. 1 (bottom). The main difference between LSDA and LDA + U occurs in the spin-down channel for the t_{2g} -like states; the d_{xy} state peels off from the d_{zx} and d_{zy} states and becomes occupied.

Experimental XMCD data are available for Fe impurity in Au.⁶ The measured value for $R_{LS} = M_L/[M_S + 7M_D] = 0.034$ is in a very good agreement with our AMF LDA + U results for U in the range between 3 and 4 eV. On the basis of these calculations we conclude that a reasonable value of the Coulomb U for Fe impurity in a Au host is ≈ 3 eV.

Our FLL results for $U = 5$ eV are fairly close to those of Ref. 4, where the LDA + U double counting was not specified. In this case, the calculated $R_{LS} = 0.21$ exceeds the experimental XMCD value by almost an order of magnitude. Therefore, the FLL LDA + U method does not satisfactorily describe the electronic structure of Fe impurity in Au.

Both the LSDA and LDA + U methods yield broken-symmetry mean-field solutions with nonzero M_S and M_L . This is because the part of the Coulomb interaction treated in the Hartree-Fock-like approximation is transformed into the exchange splitting field. This exchange field is of the order of a few eV (see Fig. 1) and by far exceeds any imaginable external magnetic field. Thus, the LDA + U method, most probably, provides a reasonable description of the local-moment systems in (strong) external magnetic fields.

When no external magnetic field is applied and no preferential direction for the orientation of the moments exists, neither LSDA nor LDA + U suffice. Recently, an attempt has been made to go beyond the static mean-field approximation and to solve the SIAM for the Fe impurity in Au employing the Hirsch-Fye quantum Monte Carlo method.⁷ The authors used a simplified three-orbital model with a diagonal Coulomb

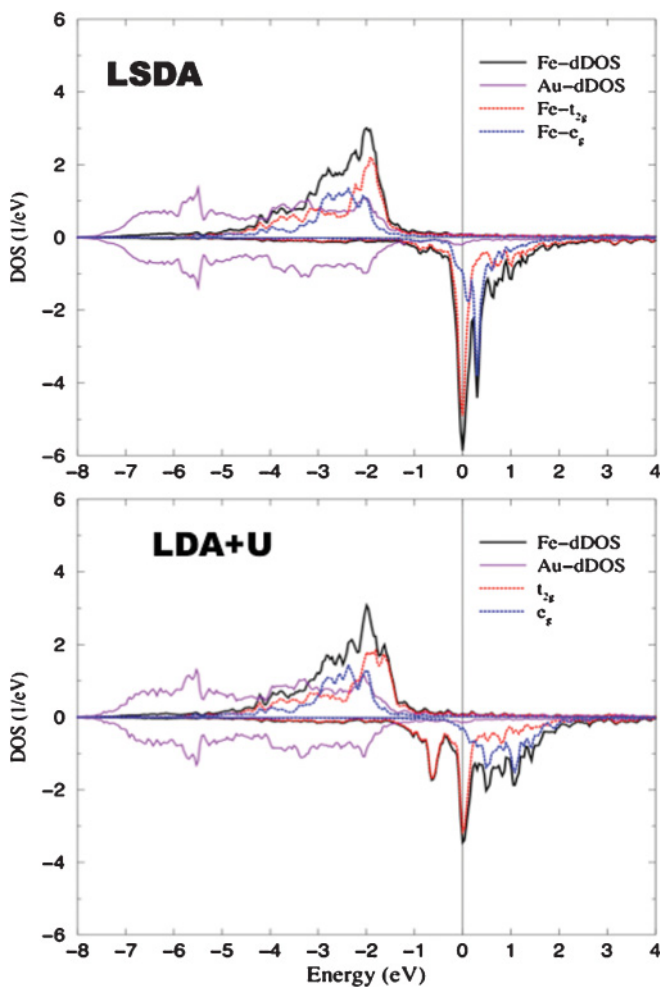


FIG. 1. (Color online) The spin-resolved d -orbital DOS for Fe impurity in Au calculated with (top) LSDA and (bottom) AMF LDA + U , $U = 3$ eV. Also shown are e_g and t_{2g} -like projected DOS for Fe.

vertex and a spin-diagonal spin-orbit coupling only. These simplifications make an estimate of the accuracy of the quantitative results reported in Ref. 7 difficult.

In order to deal with the electronic structure of the Fe impurity in the absence of the external magnetic field, we apply the finite-temperature ED method¹⁷ to the complete five-orbital d shell subject to the full spherically symmetric Coulomb interaction, spin-orbit coupling, and a cubic crystal field. The effective multiorbital impurity Hamiltonian can be written as⁹

$$\begin{aligned}
 H - \mu N = & \sum_{km\sigma} \epsilon_k b_{km\sigma}^\dagger b_{km\sigma} + \sum_{m\sigma} \epsilon_d d_{m\sigma}^\dagger d_{m\sigma} \\
 & + \sum_{mm'\sigma\sigma'} (\xi \mathbf{l} \cdot \mathbf{s} + \Delta_{\text{CF}})_{mm'}^{\sigma\sigma'} d_{m\sigma}^\dagger d_{m'\sigma'} \\
 & + \sum_{km\sigma} (V_k d_{m\sigma}^\dagger b_{km\sigma} + \text{H.c.}) \\
 & + \frac{1}{2} \sum_{\substack{mm'm'' \\ m'''\sigma\sigma'}} U_{mm'm''m'''} d_{m\sigma}^\dagger d_{m'\sigma'}^\dagger d_{m''\sigma''} d_{m'''\sigma'''} \quad (1)
 \end{aligned}$$

where $d_{m\sigma}^\dagger$ creates an electron in the d shell and $b_{km\sigma}^\dagger$ creates an electron in the “bath,” which models those host-band states that hybridize with the impurity d shell. The bath is predominantly composed of s and p bands of Au. The impurity-level position ϵ_d and the bath energies ϵ_k are measured from the chemical potential μ . Parameters ξ and Δ_{CF} specify the strength of the spin-orbit coupling and the size of the cubic crystal field on the impurity. They are determined from LDA calculations as $\xi = 60$ meV and $\Delta_{\text{CF}} = 32$ meV. The hybridization parameters V_k and the bath energies ϵ_k do not depend on m and σ . This is a good approximation for Fe in Au since the lower-symmetry components of the hybridization turn out to be considerably smaller than ξ and Δ_{CF} .

For the ED method to be applicable, the continuum of the bath states is discretized. The parameters ϵ_d , ϵ_k , and V_k are chosen so that the impurity Green’s function corresponding to the discretized Eq. (1) with $U = 0$ approximates the impurity Green’s function from the LDA as closely as possible. Namely, we require several lowest moments of the respective densities of states to coincide, $M_n^{(\text{SIAM})} = M_n^{(\text{LDA})}$, where $M_n = \int \epsilon^n g_0^d(\epsilon) d\epsilon / \int g_0^d(\epsilon) d\epsilon$.¹⁸ The integrals run over a 1-eV-wide interval centered at the Fermi level, which confines the LDA impurity resonance. The actual values of the bath parameters are $\epsilon_k^{(\text{I})} = 80$ meV and $V_k^{(\text{I})} = 220$ meV when the index k is restricted to a single value and the bath contains 10 spin-orbitals (bath I: “ $d + 10$ spin-orbitals”). For a bath twice as large we get $\epsilon_k^{(\text{II})} \in \{-310, 340\}$ meV and $V_k^{(\text{II})} \in \{140, 170\}$ meV (bath II: “ $d + 20$ spin-orbitals”). The position of the impurity level ϵ_d obtained from this procedure is subsequently shifted by a Hartree-like contribution in order to maintain the LDA impurity occupation $n_d = 6.18$ when the local Coulomb term is introduced.

After the parameters of the discrete impurity model are set, the band Lanczos method^{19,20} is utilized to determine the lowest-lying eigenstates of the many-body Hamiltonian and to calculate the one-particle Green’s function G_{SIAM}^d .

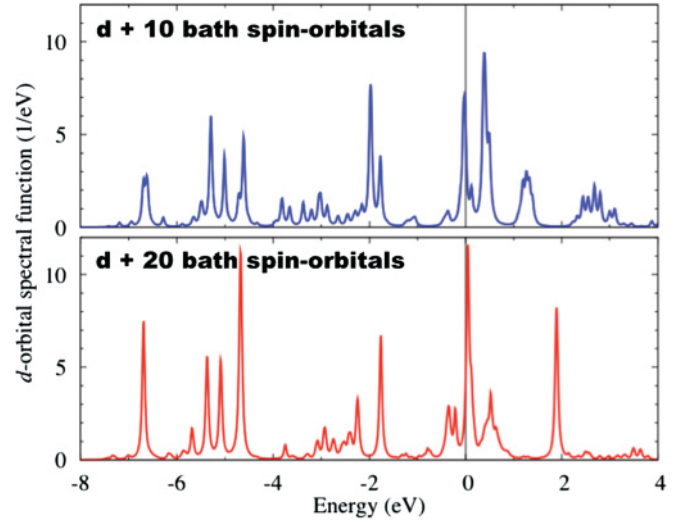


FIG. 2. (Color online) The d -electron spectral function of the impurity model of Eq. (1) with $U = 3$ eV and two variants of discrete bath: (top) 10 bath spin-orbitals and (bottom) 20 bath spin-orbitals.

The resulting d -orbital spectral function $\text{Im}(G_{\text{SIAM}}^d)/\pi$ is shown in Fig. 2 for the two models of the bath and for the Coulomb interaction parameters $U = F_0 = 3$ eV and $J = 0.9$ eV ($F_2 = 7.75$ eV, $F_4 = 4.85$ eV). The inverse temperature $\beta = 500$ eV⁻¹ was used in these calculations. Although the details of the spectral peaks depend somewhat on the particular choice of the bath, the overall structure of the spectrum with a peak(s) in the vicinity of the Fermi level is preserved when the bath parameters are varied. The spin $S = 1.91$, orbital $L = 2.21$, and total $J = 3.87$ moments are calculated for the d shell from the expectation values $\langle \hat{X}^2 \rangle = X(X + 1)$, $X = S, L, J$. Individual components of the moments, $\langle \hat{S}_z \rangle$ and $\langle \hat{L}_z \rangle$, vanish so that the spin-orbital symmetry is preserved and neither spin nor orbital polarization is induced in the absence of the external magnetic field.

Now we estimate the spin Hall angle from the skew scattering on the impurity with a local magnetic moment. Following Refs. 21 and 4, we evaluate the spin Hall angle as

$$\gamma_S \cong \frac{12\delta_1(\cos 2\delta_2^- - \cos 2\delta_2^+)}{25 - 15\cos 2\delta_2^+ - 10\cos 2\delta_2^-} \quad (2)$$

where δ_1 is the p -wave phase shift, which is assumed to be small for the nonresonant scattering, $|\delta_1| \cong 0.1$. The d -wave

TABLE III. Impurity occupations n_j and the spin Hall angle γ_S obtained with two different bath models for $U = 3$ and 5 eV. The nonmagnetic LDA calculation and an atomic-like calculation are shown for comparison.

Model	U (eV)	n_d	$n_{3/2}$	$n_{5/2}$	γ_S
LDA		6.18	2.62	3.55	0.008
Bath I	3	6.18	2.68	3.50	0.011
Bath I	5	6.18	2.85	3.33	0.021
Bath II	3	6.18	2.94	3.24	0.026
Bath II	5	6.18	2.94	3.24	0.026
No bath	3–5	6.18	2.98	3.19	0.029

phase shifts δ_2^+ for $j = 5/2$ and δ_2^- for $j = 3/2$ are related to the occupations $n_{3/2}$ and $n_{5/2}$ of the corresponding $3d$ subshells via the Friedel sum rule $\delta_2^{(j)} = \pi n_j / (2j + 1)$.⁹ The Hall angle γ_S vanishes when all d orbitals are equally occupied ($\delta_2^- = \delta_2^+$), it grows as an increasing spin-orbit coupling favors the occupation of the $j = 3/2$ subshell, and it eventually reaches a maximum $\gamma_S^{(\max)} = 4\delta_1/5$ when the $j = 3/2$ subshell is completely filled ($n_{3/2} = 4$ and $\delta_2^- = \pi$).

The occupation numbers n_j and the Hall angle γ_S obtained for the Hamiltonian of Eq. (1) are listed in Table III for the two bath models introduced earlier and for $U = 3$ and 5 eV. Results of the nonmagnetic LDA calculation and of an atomic-like calculation without any bath orbitals are shown for comparison. The angle γ_S increases when the Coulomb U is added and keeps growing with further increase of U . For a fixed value of U , the Hall angle decreases with increasing hybridization V since the spin-orbit splitting in the host band is negligible, and the hybridization thus effectively reduces the spin-orbit effects in the Fe d shell.

Our results are consistent with the measurements of Fert *et al.*²² of the anomalous Hall coefficient of ~ 0.01 in dilute $3d$ noble metal alloys. The angle $\gamma_S \approx 0.025$ we obtain is 50% smaller than the earlier theoretical estimate $\gamma_S = 0.055$ by Gu *et al.*⁷ and substantially smaller than the “giant” $\gamma_S = 0.11$ reported by Seki *et al.*³ Note that the results of Ref. 3 were very recently reexamined in Ref. 23, where it was shown that the increase of Au-Hall cross thickness from 10 to 20 nm

substantially reduces the spin Hall angle. Moreover, very recent calculations²⁴ proposed that light impurities, C, N, and Ar, can lead to a substantial enhancement of the spin Hall effect in gold, and hence the observed Hall angle could be an effect of sample contamination. Thus the existence and origin of a “giant” spin Hall effect in Au remains controversial.

To summarize, our calculations show that the AMF LDA + U method with the Coulomb U around 3 eV reproduces very well the XMCD experimental data for Fe impurity in an Au host. The calculated orbital moment at the Fe atom, $M_L = 0.16 \mu_B$, is almost ten times smaller than that reported by Guo *et al.*⁴ We explicitly show that the reason for this difference is not only in the use of a smaller value of U (Ref. 7) but also in the appropriate choice of the LDA + U flavor. Furthermore, using the exact diagonalization of a multiorbital impurity model, we estimate the spin Hall angle due to the scattering on the Fe impurity in the Au host as $\gamma_S \approx 0.025$. It is substantially smaller than $\gamma_S = 0.11$ reported by Seki *et al.*³ We conclude that scattering of Fe impurities in Au does not yield a giant SHE.

We acknowledge stimulating discussions with T. Jungwirth, J. Wunderlich, J. Sinova, and I. Mertig and financial support from Czech Republic Grants No. GACR P204/10/0330, No. GAAV IAA100100912, and No. AV0Z10100520. J.K. acknowledges support by the Alexander von Humboldt foundation.

¹Y. K. Kato, R. S. Myers, A. C. Gossard, and D. D. Awschalom, *Science* **306**, 1910 (2004); J. Wunderlich, B. Kaestner, J. Sinova, and T. Jungwirth, *Phys. Rev. Lett.* **94**, 047204 (2005).

²S. O. Valenzuela and M. Tinkham, *Nature (London)* **442**, 176 (2006).

³T. Seki *et al.*, *Nat. Mater.* **7**, 125 (2008).

⁴G. Y. Guo, S. Maekawa, and N. Nagaosa, *Phys. Rev. Lett.* **102**, 036401 (2009).

⁵T. Costi *et al.*, *Phys. Rev. Lett.* **102**, 056802 (2009).

⁶W. D. Brewer, A. Scherz, C. Sorg, H. Wende, K. Baberschke, P. Bencok, and S. Frota-Pessoa, *Phys. Rev. Lett.* **93**, 077205 (2004).

⁷B. Gu, J. Y. Gan, N. Bulut, T. Ziman, G. Y. Guo, N. Nagaosa, and S. Maekawa, *Phys. Rev. Lett.* **105**, 086401 (2010).

⁸A. I. Liechtenstein, V. I. Anisimov, and J. Zaanen, *Phys. Rev. B* **52**, R5467 (1995).

⁹A. C. Hewson, *The Kondo Problem to Heavy Fermions* (Cambridge University Press, Cambridge, 1993).

¹⁰A. B. Shick and W. E. Pickett, *Phys. Rev. Lett.* **86**, 300 (2001).

¹¹V. von Barth and L. Hedin, *J. Phys. C* **5**, 1629 (1972).

¹²A. B. Shick, D. L. Novikov, and A. J. Freeman, *Phys. Rev. B* **56**, R14259 (1997).

¹³S. Frota-Pessoa, *Phys. Rev. B* **69**, 104401 (2004).

¹⁴S. Chadov *et al.*, *Europhys. Lett.* **82**, 37001 (2008).

¹⁵R. Wu and A. J. Freeman, *Phys. Rev. Lett.* **73**, 1994 (1994).

¹⁶F. Bultmark, F. Cricchio, O. Granas, and L. Nordstrom, *Phys. Rev. B* **80**, 035121 (2009).

¹⁷J. Kolorenč (unpublished).

¹⁸A. Georges *et al.*, *Rev. Mod. Phys.* **68**, 13 (1996).

¹⁹A. Ruhe, *Math. Comput.* **33**, 680 (1979).

²⁰H.-D. Meyer and S. Pal, *J. Chem. Phys.* **91**, 6195 (1989).

²¹H.-A. Engel, B. I. Halperin, and E. I. Rashba, *Phys. Rev. Lett.* **95**, 166605 (2005).

²²A. Fert, A. Friedrich, and A. Hamzic, *J. Magn. Magn. Mater.* **24**, 231 (1981).

²³T. Seki *et al.*, *Solid State Commun.* **150**, 496 (2010).

²⁴M. Gradhand, D. V. Fedorov, P. Zahn, and I. Mertig, *Phys. Rev. Lett.* **104**, 186403 (2010).